Design Optimization of a Direct-drive Wind Generator with Non-rare-earth PM Flux Intensifying Stator and Reluctance Rotor

Ali Mohammadi, Oluwaseun A. Badewa, Yaser Chulaee, Dan M. Ionel,
Somasundaram Essakiappan[1], and Madhav Manjrekar[1]
SPARK Laboratory, ECE Department, University of Kentucky, Lexington, KY, USA
[1]QM Power, Inc., Charlotte, NC, USA
alimohammadi@uky.edu, o.badewa@uky.edu, yaser.chulaee@uky.edu, dan.ionel@ieee.org,
somasundaram@qmpower.com, mmanjrekar@qmpower.com

***Abstract*— This paper presents a multi-objective design optimization for a novel direct-drive wind turbine generator. The proposed electric machine topology employs an outer rotor of the reluctance type and a special modular stator including three phase-windings and spoke-type permanent magnets (PMs). Each stator module includes a single coil toroidally wound around the ferromagnetic core. Consecutive stator modules are separated by PMs and include coils belonging to a different phase. An optimization method with three objectives: total power loss, weight, and torque ripple, and with one constraint for a minimum acceptable value for the power factor, is described. The design examples are for a direct-drive generator rated at 3 MW and 15 rpm. The simulation results show that with the proposed topology, which greatly benefits from PM flux concentration and special coils, performance, such as specific thrust, efficiency, "goodness", etc, can be comparable to more traditional synchronous PM designs, but without the need to use rare earth-magnets that have high cost and critical supply. Furthermore, options for using aluminum instead of copper wire to further reduce the weight and cost of winding are investigated and comparative results are discussed.**

***Index Terms*—Direct-drive generator, wind turbine, multi-objective optimization, electric machine, FEA, flux-intensifying topology, reluctance rotor.**

I. Introduction

Wind power has the potential to significantly reduce greenhouse gas emissions, making it an attractive option for countries looking to mitigate the effects of climate change. The growing demand for energy has prompted a significant shift towards renewable energy sources, with wind power being a particularly popular source, with continuously increasing installed capacity. In fact, wind energy has been identified as one of the fastest-growing sources of renewable energy [1].

The International Energy Agency projects that renewable energy generation is forecasted to provide 30% of global electricity by 2024, and global renewable energy capacity is expected to increase by almost 2400 GW (75%) between 2022 and 2027. Furthermore, the global annual installations of onshore and offshore wind power are predicted to increase by almost 50% in 2027 [2].

Traditional wind turbines have an electric generator, a gearbox with more than one stage, and a power electronic converter. The gearbox serves to step up the speed of the turbine to a synchronous speed that fits with the generator. It has been reported that gearboxes are one of the most expensive parts of offshore wind turbines and could be associated with failures and the resulting operational downtime [3–5].

Direct-drive wind turbines have become a promising and more efficient alternative to traditional wind turbines by eliminating the gearbox, resulting in higher reliability and reduced maintenance costs. Additionally, eliminating the gearbox also reduces noise and vibration levels, making direct-drive turbines a preferred choice for onshore and offshore wind power installations [6, 7]. The reduction in maintenance requirements in direct-drive wind turbines is considered a crucial accomplishment, particularly for offshore wind turbines [8].

Direct-drive wind turbines often feature unique design concepts, such as spoke permanent magnets [1]. This type of design allows for increased power density and improved performance [9], which is crucial because eliminating the gearbox causes the generator to rotate at low speeds. This, in turn, significantly increases the generator volume and weight and as a result, a stronger and more expensive tower structure is required for direct-drive wind turbines.

In a previous paper [1], we introduced the concept of a new generator design illustrated in Fig. 1a; and this concept features spoke permanent magnets, which allows for a high flux concentration ratio. The aforementioned paper provides an in-depth understanding of its fundamental operation, along with a detailed analysis of the underlying equations. Additionally, we conducted a comprehensive parametric study to explore the potential of this flux-intensifying generator. Building upon our previous work, to ensure the satisfactory performance of the generator and effective use of active materials, this current paper presents further contributions to the under-study generator

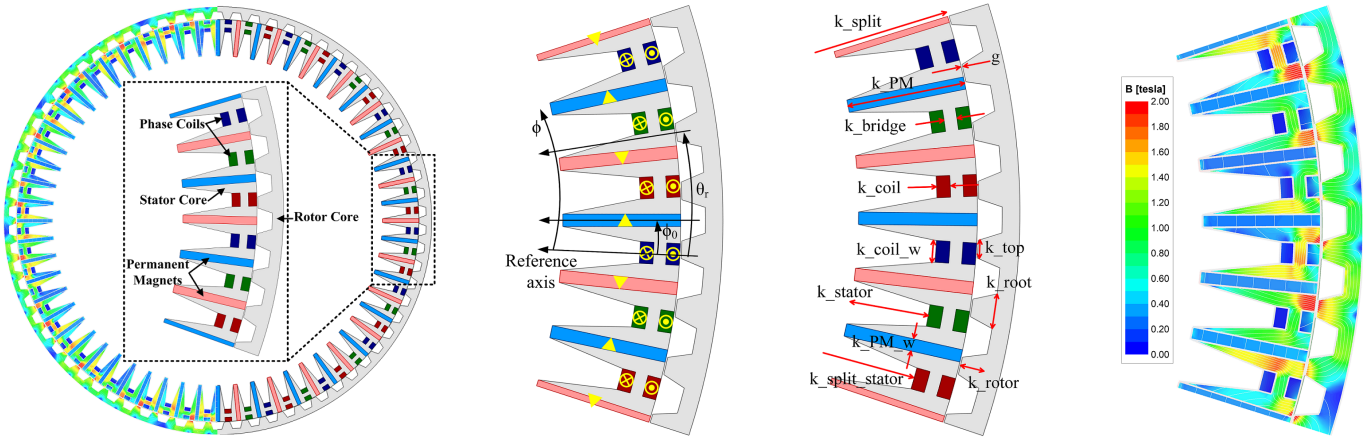

(a) (b) (c) (d)

Fig. 1. (a) The cross-section, and enlarged detailed view of the direct drive generator topology, (b) the cross-section of the smaller periodicity region for the example generator design with 7 rotor protrusions, (c) geometric design variables used in the parametric model in the multi-objective optimization of the under-study generator, and (d) magnetic flux density and flux line distribution of the direct drive wind generator concept.

and specifically, focuses on a systematic design optimization to enhance the generator's performance and reduce the cost of materials, especially permanent magnets.

The dimensions and performance indices of three direct-drive wind generators, which employ rare-earth NdFeB permanent magnets are summarized in Table I. The cost of this type of permanent magnet is high, and in applications such as direct-drive wind turbines, where the electric machine diameter is very large, it is important to perform an optimization on the design to reduce the cost of material as much as possible. Another method to reduce the material cost is to use non-rare-earth permanent magnets that have a lower cost compared to their rare-earth counterparts.

The topology to be optimized in this paper is suitable for the aforementioned method, in which the stator's PMs are arranged in a spoke-like configuration, substantially intensifying the flux and allowing the use of non-rare-earth PMs. Furthermore, this design allows for a higher flux concentration in the air gap, leading to a high specific torque and power generator. The combination of spoke magnets and slots with relatively large width implicitly creates in the stator a structure with flux barriers, which may be beneficial for high torque density, as it was previously proposed and demonstrated for the rotors of IPM synchronous motors [10].

Direct drive generators as mentioned previously, are known for their inherently heavy weight, which has prompted researchers to explore alternative solutions. In this paper, a study has been performed to further reduce the weight after the selection of the optimized design. In this study, copper windings are replaced with aluminum windings. The use of aluminum winding can result in a significant weight reduction of the generator winding without compromising its performance.

II. Wind Turbine Generator Topology and Principle of Operation

The generator being studied was structured as shown in Fig. 1. Each segment of the stator includes a permanent magnet and a single concentrated coil that belongs to a phase winding. The stator core has modular slots that allow the use of rectangular wire, leading to a high slot fill factor and reduced copper losses. Additionally, the concentrated coils have compact axial ends that are toroidally wound, further reducing copper losses. This topology utilizes stator PMs that separate modules of the core and concentrated AC coils toroidally wound around the back iron, resulting in a high winding factor, as discussed for example in [13].

The effectiveness of an electric machine's winding can be comparable to that of a fully pitched winding, depending on the machine's proportions, such as airgap diameter and stack length. To maximize the advantages, it is beneficial to ensure that the coils' return path is positioned outside the back iron, rather than along the circumferential direction with typical end coils. In cases where the machine's proportions are substantial, having end coils along the circumferential direction would result in a substantially longer return path, leading to increased losses and weight. Therefore, careful consideration of coil placement is necessary to optimize the efficiency and performance of electric machines.

The wind turbine designed in this paper utilizes a winding pattern that is linked to the arrangement of the three phases at the stator's periphery. With only one coil side inserted into each slot, this configuration offers substantial fault tolerance. Additionally, the permanent magnets are situated radially in the stator and are magnetized in opposite tangential directions. The magnets are capable of extending significantly in the radial direction, allowing for particularly high flux concentration and airgap flux densities.

The rotor features a laminated steel core of the reluctance type with protrusions whose number and dimensions are coordinated with the characteristics of the stator. For the proposed concept, Fig. 1b depicts the analyzed minimal region of periodicity, which includes seven rotor protrusions. This section was replicated 10 times to create the full generator cross-section, which has hence 70 rotor protrusions corresponding to 140 magnetic poles. The core material used in this design was M19. The open-circuit (OC) PM field and the armature field

Table I
SUMMARY OF MAIN DIMENSIONS AND PERFORMANCE FOR PM (NDFEB TYPE) DIRECT-DRIVE WIND TURBINE GENERATORS.

Ref.	Output Power [MW]	Airgap diameter [m]	Stack length [m]	Efficiency [%]	Specific PM mass [g/Nm]	Specific total mass [g/Nm]	Specific thrust [kN/m2]	Goodness [kNm/$\sqrt{W_{loss}}$]
[11]	3.0	5.0	1.9	95.9	1.451	N/A	25.867	5.622
[11]	3.1	5.0	1.9	97.2	1.793	N/A	26.537	6.620
[12]	3.0	4.7	1.2	96.0	0.895	12.684	44.864	5.374

are examined using the MMF-permeance model presented in [1] to describe the working principle of the presented generator concept and the torque generation process.

To examine the OC PM field, the armature windings were disregarded, leaving the PMs as the sole magnetic field source, and to study the armature windings field the permanent magnets were disregarded. The airgap flux density distribution created by PMs can be computed without considering the influence of stator slotting. The airgap flux density distribution created by armature winding can be computed similarly. Adjacent PMs were magnetized in different directions, as seen in Fig. 1b, resulting in significant flux concentration. The electromagnetic performance of the machine can be determined by the arrangement of stator permanent magnets, rotor protrusions, and stator toroidal coils according to [14].

III. PROBLEM FORMULATION

The target power and speed requirements for the direct drive wind turbine topology under investigation were 3 MW and 15 rpm, respectively. Detailed optimization of the proposed design was carried out considering the farthest geometrically and mechanically stable limits that would maximize the set objective functions. The limits of the variables were not set based on a reference design but rather through parametric studies to ensure a wide optimization area. The outer diameter, current density as well as the number of poles are kept constant while other variables are systematically analyzed to target the most favorable design.

The three concurrent objectives of the optimization are to *minimize* the total power loss F_1, total active mass F_2, and torque ripple F_3:

$$\begin{aligned} F_1 &= P_{Total} = P_{Fe} + P_{Cu}, \\ F_2 &= M_{Total} = M_{Stator} + M_{Rotor}, \\ F_3 &= T_{Ripple} = \frac{T_{\max} - T_{\min}}{T_{avg}} \times 100\%, \end{aligned} \tag{1}$$

with an additional *constraint* on the power factor to a minimum value of 0.7. The objective function for total power loss was calculated as the sum of the variable and constant losses of the generator, where P_{Fe} represents the core loss (constant losses) and P_{Cu} represents the copper loss (variable losses). The objective function for total active mass considers the mass of active components, including the stator M_{Stator} and the rotor M_{Rotor}, where the stator mass includes its core mass, the mass of its winding, and the mass of permanent magnets. Torque ripple is calculated by dividing the difference of the maximum of the electromagnetic torque T_{max}, and its minimum T_{min} by its average T_{avg}.

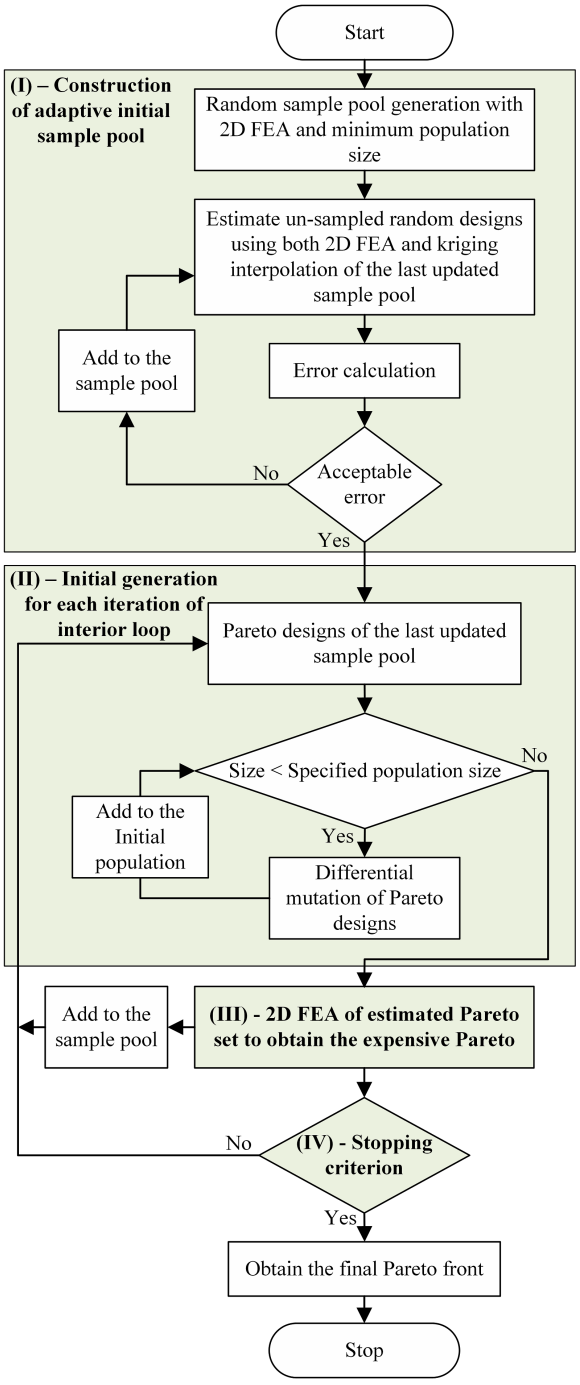

Fig. 2. The two-level optimization algorithm with an interior loop based on differential evolution method.

The first step of the optimization algorithm was to generate an initial design pool as shown in the optimization algorithm

Table II
INDEPENDENT VARIABLES FOR THE OPTIMIZATION, THEIR DESCRIPTION BASED ON DESIGN SPECIFICATIONS, AND CORRESPONDING VALUES.

Variable	Description	Min	Max
g	airgap [mm]	5.00	6.00
k_split	split ratio = $\frac{ID_r}{OD_r}$	0.90	0.98
k_PM	PM length ratio = $\frac{\ell_{PM}}{OD_s - ID_s}$	0.80	1.20
k_PM_w	PM width ratio = $\frac{w_{PM}}{\tau_s}$	0.10	0.35
k_bridge	bridge length ratio = $\frac{\ell_b}{\tau_s}$	0.20	0.45
k_slot	slot length ratio = $\frac{\ell_{slot}}{OD_s - ID_s}$	0.30	0.75
k_slot_w	slot width ratio = $\frac{w_{slot}}{\tau_s}$	0.10	0.35
k_top	rotor pole top ratio = $\frac{\tau_{rpt}}{\tau_r}$	0.30	0.70
k_root	rotor pole root ratio = $\frac{\tau_{rpr}}{\tau_r}$	0.30	0.70
k_split_stator	stator split ratio = $\frac{ID_s}{OD_s}$	0.90	0.98
k_stator	stator extension ratio = $\frac{\ell_{se}}{OD_s - ID_s}$	0.75	0.85
k_rotor	rotor pole depth ratio = $\frac{\ell_{rpd}}{OD_r - ID_r}$	0.30	0.70

flowchart depicted in Fig. 2. There are different methods to accomplish this, including using randomized designs or design of experiments (DoE). In this study, random designs were implemented to generate the initial design pool. This was because DoE requires a high number of designs to account for non-linearities in optimization problems with a larger design space and more variables. Since this study dealt with such a problem, it was more practical to use random designs.

After the initial design pool was generated, the next step was to increase the resolution of the design pool in promising regions of the search space. This was because a higher resolution of design points in these regions would result in a better understanding of the behavior of the optimization problem in those areas. On the other hand, regions of the search space that do not show promise can be sampled less frequently. By doing so, computational resources can be utilized more effectively, and the search process can be made more efficient.

Multi-objective optimizations often employ termination criteria to determine when to stop the optimization process. In our case, a hybrid stopping criterion was used that took into account the convergence of the optimization algorithm where the termination criterion was either a maximum number of generations or a minimal improvement in three representative points of the Pareto front for a few consecutive generations [15].

In this paper, twelve geometrical variables were chosen as optimization variables, as shown in Fig. 1c and Table II shows the description of the variables and the selected range. The range of the independent variables was selected through the design of the experiment to have the most effective parameters and also avoid geometrical errors during the optimization process. Only the air gap had an absolute value expressed in "mm". Through the use of a two-pass study, it was made certain that each design was capable of producing the rated torque at the rated speed. In the first step of the process, a predetermined stack length was used to examine the design. The stack length was then scaled based on the produced torque and the specified torque, and the design was re-evaluated to ensure that the rated torque was obtained.

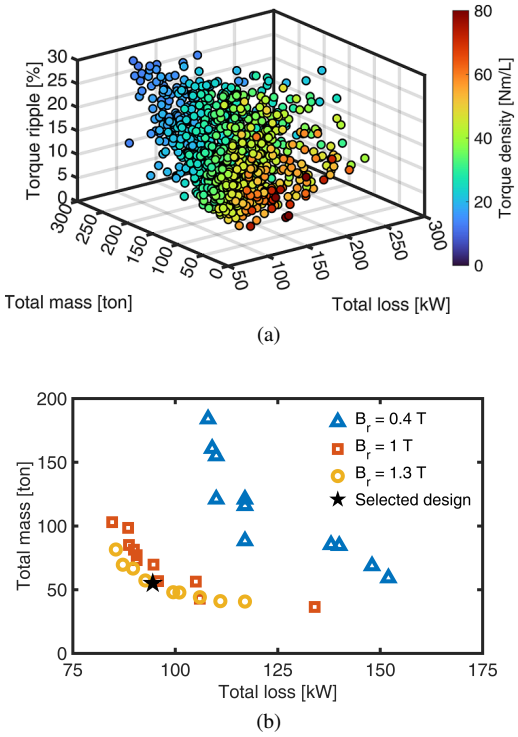

Fig. 3. (a) The results of the multi-objective optimization for PM with B_r equal to 1 T, (b) Pareto optimal designs of optimization results of PMs with different remanent flux densities.

IV. OPTIMIZATION RESULTS, DESIGN VARIATIONS, AND DISCUSSION

The optimization process was carried out using the under-investigation topology by exploring a range of permanent magnet materials, each with a unique remanent flux density (B_r). To this end, non-rare earth PMs with B_r values of 0.4 and 1 T, as well as rare-earth magnetic materials with B_r equal to 1.3 T were examined. In each scenario, a population size of fifty different designs per generation was utilized to ensure an extensive exploration of the design space. To evaluate the performance of the generated designs, 2D-FEA simulations were conducted using Ansys Electronics 2022 software [16].

The outcomes of the optimization process for each condition are depicted in Figs. 3 and 4. According to the results, when employing non-rare earth permanent magnet material with a remanent flux density of 0.4 T, as shown in Fig. 4a, the optimal design, in order to have a low torque ripple, total losses, and a high power factor, trends to have a higher total mass. The power factor reported for the majority of the designs has high values and in some designs close to unity. Also, by considering the minimum total mass, total losses, and torque ripple, the best designs for B_r= 1 T are shown as an example in Fig. 3a, indicating that the best designs have high torque density, which is in line with expectations.

The Pareto fronts of the optimal designs of the three materials used for the wind generator under study are combined and depicted in Fig. 3b. The results show that the Pareto fronts of the optimal designs using permanent magnets with a remanent flux density of 0.4 T are clearly distinguished from generators

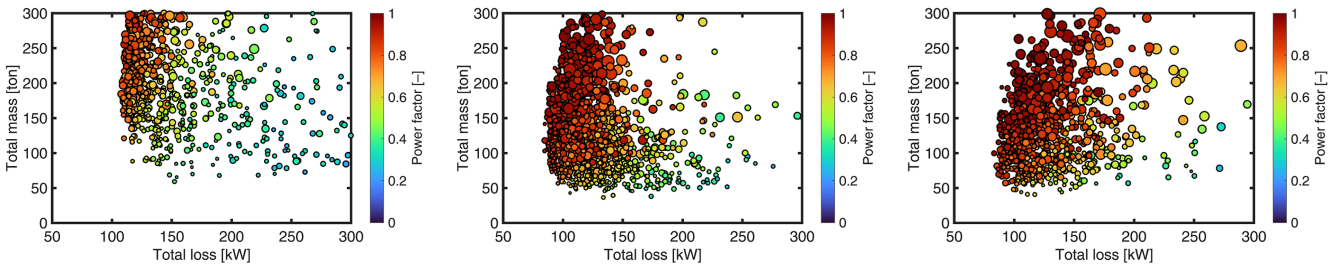

Fig. 4. Results of the multi-objective optimization showing the design distribution considering the total mass, total loss, power factor, and torque ripple for the generators using, (a) B_r= 0.4 T, (b) B_r=1 T, and (c) B_r= 1.3 T. The size of the circle marker for each design is proportional to the torque ripple.

Table III
PERFORMANCE COMPARISON OF THE OPTIMAL DESIGNS: DESIGNS A AND B ARE THE BEST DESIGNS WITH RARE-EARTH PERMANENT MAGNETS AND DESIGNS C AND D ARE THE BEST DESIGNS WITH NON-RARE-EARTH PERMANENT MAGNETS. THE RATED POWER OF THE OPTIMIZATION IS 3 MW, AND THE SPEED IS 15 RPM.

Design ID	Airgap diameter [m]	Stack length [m]	Electromagnetic efficiency [%]	Power factor [–]	Torque density [Nm/L]	Specific thrust [kN/m^2]	Goodness [kNm/$\sqrt{W_{loss}}$]
Best designs with **non-rare-earth** permanent magnets (B_r = 1 T)							
A	4.7	1.7	96.9	0.76	52.5	32.180	6.173
B	4.8	1.7	96.6	0.67	52.0	31.440	5.902
Best designs with **rare-earth** permanent magnets (B_r = 1.3 T)							
C	4.7	2.1	97.1	0.90	43.8	34.857	6.380
D	4.7	2.0	97.2	0.90	45.2	36.432	6.473

that use PMs with a B_r of 1 and 1.3 T. Results indicate that by utilizing a flux-intensifying topology with non-rare earth permanent magnets having a remanence of 1 T, such as high-energy non-rare earth PMs produced by the company Niron Magnetics [17], it is possible to achieve comparable performance to direct-drive generators that employ rare-earth permanent magnets, as investigated in the literature reported in Table I. This represents a significant improvement facilitated by the flux-intensifying topology described in this study, which allows for similar performance to be obtained while utilizing significantly less expensive permanent magnet materials.

The ability of the proposed topology to make use of non-rare earth permanent magnets can significantly reduce the cost of permanent magnet materials in this application, which requires a significant amount of PMs. Two of the best design topologies that employ PMs with a remanence of 1 and 1.3 T, selected through optimization, are depicted in Fig. 5.

A comprehensive comparison of the geometrical and performance indices of the best designs on the Pareto, as presented in Fig. 5, is provided in Table III. The table indicates that achieving comparable performance between non-rare-earth permanent magnet materials and their rare-earth counterparts is feasible. The example designs are marked with a star on the Pareto shown in Fig. 3b. The non-rare earth optimum design A, for example, has a goodness of 6.173 kNm/$\sqrt{W_{loss}}$, and a specific thrust of 32.180 [kN/m^2], which are comparable to the designs reported in the literature reported in Table I, that use expensive and high remanence PMs.

The substitution of copper with aluminum in the armature windings of wind turbines is a topic of considerable interest since it can contribute to the reduction of material costs and weight. The difference in mass density between copper and

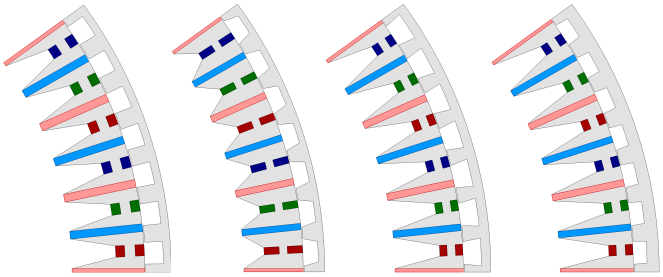

Fig. 5. Schematic of the optimized design topologies: (a) and (b) use non-rare earth materials, (c) and (d) use rare earth materials. Larger copper area in the non-rare-earth topologies shows the compensation for non-rare earth versus rare-earth materials.

aluminum is significant, with aluminum having a density that is approximately one-third that of copper. Therefore, replacing copper with aluminum can result in a significant reduction in the weight of the wind turbine generator, which can lead to a reduction in the cost of materials and potentially lower the cost of power generated by the turbine.

To investigate the effect of aluminum windings on the performance of wind turbines, an optimized design topology was selected and modified by replacing the copper windings with aluminum. It was important to ensure that the substitution of materials did not compromise the performance of the wind turbine generator. Therefore, the modified design topology was carefully designed to maintain a similar level of performance to the original design.

To compensate for the difference in conductivity between copper and aluminum, the coil slot area was almost doubled, as shown in Fig. 6. This modification helped to ensure that the aluminum windings could provide similar electrical

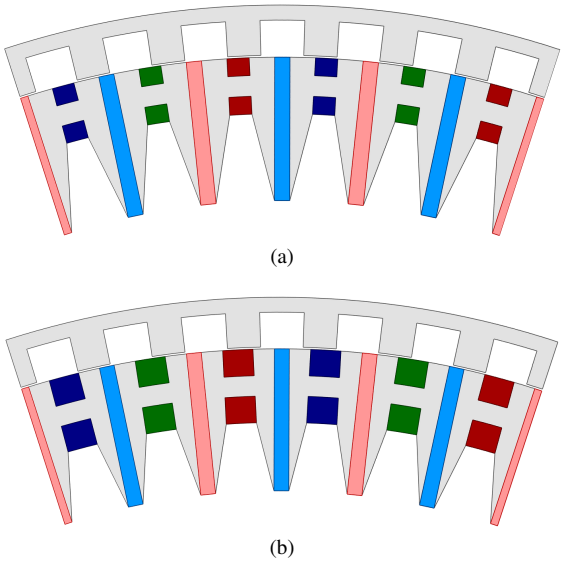

(a)

(b)

Fig. 6. Schematic of the optimized design "A" topology using non-rare earth material with, (a) copper winding, and (b) aluminum winding.

performance to the original copper windings. As a result of this modification, the weight of the armature windings was reduced by 36%, which is a substantial improvement in terms of material cost and weight reduction.

V. Conclusion

To improve the performance of a novel concept of a direct-drive wind turbine electric generator, a large-scale, multi-objective design optimization relying on FEA was carried out, involving numerous independent variables and three concurrent objectives with one constraint for a minimum acceptable value for the power factor. In this study, three different magnetic materials were considered, and their Pareto fronts were compared. The optimal designs with the proposed flux-intensifying topology and toroidal coils that use non-rare-earth PMs with a remanence of B_r= 1T can deliver comparable performance to their counterpart employing expensive rare-earth PMs which are prone to availability/supply chain risks. These designs have been systematically compared considering performance indices such as specific thrust and machine goodness. Also, the optimal designs are characterized by low torque ripple, below 10%, and high power factor. Upon further investigation, using aluminum instead of copper in the stator winding resulted in a 36% weight reduction. These findings highlight the potential of such optimizations in achieving high-performance, cost-effective designs for wind turbine electric generators.

Acknowledgements

This paper is based upon research sponsored by the QM Power Inc. The support of ANSYS Inc., and University of Kentucky, the L. Stanley Pigman Chair in Power Endowment is also gratefully acknowledged.

References

[1] A. Mohammadi, O. A. Badewa, Y. Chulaee, D. M. Ionel, S. Essakiappan, and M. Manjrekar, "Direct-drive wind generator concept with non-rare-earth pm flux intensifying stator and reluctance outer rotor," in *2022 11th International Conference on Renewable Energy Research and Application (ICRERA)*. IEEE, 2022, pp. 582–587.

[2] International Energy Agency, *Renewables 2022: Analysis and forecast to 2027*. Paris, France: OECD/IEA, 2022. [Online]. Available: https://www.iea.org/reports/renewables-2022

[3] H. Chen, A. M. EL-Refaie, Y. Zuo, S. Cai, J. Tang, Y. Liu, and C. H. T. Lee, "A permanent magnet brushless doubly-fed electric machine for variable-speed constant-frequency wind turbines," *IEEE Transactions on Industrial Electronics*, pp. 1–12, 2022.

[4] H. S. Dhiman, D. Deb, S. M. Muyeen, and I. Kamwa, "Wind turbine gearbox anomaly detection based on adaptive threshold and twin support vector machines," *IEEE Transactions on Energy Conversion*, vol. 36, no. 4, pp. 3462–3469, 2021.

[5] H. Dastres, A. Mohammadi, and B. Rezaie, "Adaptive robust control design to maximize the harvested power in a wind turbine with input constraint," *Journal of Renewable Energy and Environment*, vol. 7, no. 4, pp. 30–43, 2020.

[6] F. Blaabjerg and D. M. Ionel, *Renewable energy devices and systems with simulations in matlab® and ansys®*. CRC Press, 2017.

[7] R. Nasiri-Zarandi, A. M. Ajamloo, and K. Abbaszadeh, "Design optimization of a transverse flux halbach-array pm generator for direct drive wind turbines," *IEEE Transactions on Energy Conversion*, vol. 35, no. 3, pp. 1485–1493, 2020.

[8] N. A. Bhuiyan and A. McDonald, "Optimization of offshore direct drive wind turbine generators with consideration of permanent magnet grade and temperature," *IEEE Transactions on Energy Conversion*, vol. 34, no. 2, pp. 1105–1114, 2019.

[9] A. Mohammadi and S. M. Mirimani, "Design and analysis of a novel permanent magnet assisted synchronous reluctance machine using finite-element-method," in *2020 11th Power Electronics, Drive Systems, and Technologies Conference (PEDSTC)*, 2020, pp. 1–5.

[10] D. M. Ionel, J. F. Eastham, and T. Betzer, "Finite element analysis of a novel brushless dc motor with flux barriers," *IEEE Transactions on Magnetics*, vol. 31, no. 6, pp. 3749–3751, 1995.

[11] M. Lehr, D. Dietz, and A. Binder, "Electromagnetic design of a permanent magnet flux-switching-machine as a direct-driven 3 mw wind power generator," in *2018 IEEE International Conference on Industrial Technology (ICIT)*. IEEE, 2018, pp. 383–388.

[12] H. Polinder, F. F. Van der Pijl, G.-J. De Vilder, and P. J. Tavner, "Comparison of direct-drive and geared generator concepts for wind turbines," *IEEE Transactions on energy conversion*, vol. 21, no. 3, pp. 725–733, 2006.

[13] G. Heins, D. M. Ionel, and M. Thiele, "Winding factors and magnetic fields in permanent-magnet brushless machines with concentrated windings and modular stator cores," *IEEE Transactions on Industry Applications*, vol. 51, no. 4, pp. 2924–2932, 2015.

[14] P. Han, M. G. Kesgin, D. M. Ionel, R. Gosalia, N. Shah, C. J. Flynn, C. S. Goli, S. Essakiappan, and M. Manjrekar, "Design optimization of a very high power density motor with a reluctance rotor and a modular stator having pms and toroidal windings," in *2021 IEEE Energy Conversion Congress and Exposition (ECCE)*, 2021, pp. 4424–4430.

[15] M. Rosu, P. Zhou, D. Lin, D. M. Ionel, M. Popescu, F. Blaabjerg, V. Rallabandi, and D. Staton, *"Multiphysics Simulation by Design for Electrical Machines, Power Electronics and Drives"*, J. Wiley - IEEE Press, 2017.

[16] *Ansys® Electronics, version 22.1, 2022, ANSYS Inc.*

[17] Niron Magnetics, *Niron Magnetics: Magnets Rare Earth vs Clean Earth*, Minneapolis, Minnesota, USA, 2023. [Online]. Available: https://www.nironmagnetics.com/#OurTechnology